Functional Gene and Metabolic Changes of Marine Microbial Populations Involved in Hydrocarbon Degradation Under Different Enrichment Conditions

Bingkui Song
Hebei University of Technology
Zhongzhen Zhang
Hebei University of Technology
Si Li (jackeikee@126.com)
Hebei University of Technology https://orcid.org/0000-0001-9138-3569
Qitong Fu
Hebei University of Technology
Shuting Qi
Hebei University of Technology
Liang Li
Hebei University of Technology
Di Mu
Hebei University of Technology
Aili Zhang
Hebei University of Technology

Research Article

Keywords: Marine microorganisms, Petroleum hydrocarbon degradation, Metatranscriptome, KEGG pathway enrichment analysis, Metabolic Pathway

Posted Date: April 27th, 2021

DOI: https://doi.org/10.21203/rs.3.rs-457199/v1

Abstract

In this study, seawater from the area of an oil extraction platform in Bohai Bay was subjected to experimental treatments with oil as the only carbon source to understand the transcriptional responses of seawater microbial populations to oil degradation treatments. Twelve enrichment conditions were used, and fluorescent in situ hybridization (FISH) along with metatranscriptomic analyses were used to understand functional changes within each treatment. RNA from the petroleum-degrading bacterial enrichments was extracted after cultivation and FISH was used to evaluate overall activity, while changes in gene expression among different culture conditions were analyzed based on eight hydrocarbon-specific gene probes and flow cytometry. Concomitantly, 1,066 metabolic pathways were identified as being expressed in the populations through RNA sequencing, metatranscriptomic analysis, and metabolic pathway enrichment analysis. The addition of oil led to the inhibition of carbohydrate metabolism and inositol phosphate metabolism, while also reducing extracellular signaling pathway transcription levels. When low- and high-nutrient conditions were compared, low-nutrient conditions inhibited taurine and hypotaurine metabolism in addition to inositol phosphate metabolism. Among oxygen-treated, carbon dioxide-treated, and air-treated conditions, oxygen-treated conditions inhibited taurine and hypotaurine metabolism but promoted galactose metabolism, while carbon dioxide-treated conditions promoted inositol phosphate metabolism. Overall, metabolic pathway expression and functional gene changes indicated that high-nutrient, oil-free, and aerobic culture conditions best promoted the growth and reproduction of marine microbial communities.

Introduction

Marine pollution caused by offshore oil exploitation is one of the most important challenges for modern environments. However, microbial oil degradation offers unique advantages for the prevention and treatment of offshore oil pollution due to the low cost of application, high efficiency of degradation activity, and minimal pollution risk [1, 2]. Dehydrogenation, hydroxylation, and hydroperoxidation activities by microorganisms lead to the breakdown of alkanes and aromatic hydrocarbons in petroleum that are then used in the tricarboxylic acid cycle, transforming the carbon to CO_2 and water while simultaneously promoting energy conservation within microbial populations [3, 4]. Environmental variation can significantly impact the ability of microorganisms to degrade petroleum hydrocarbons, and these degradation efficiencies can greatly vary across environments. If environmental parameters inhibit the growth of petroleum hydrocarbon-degrading bacteria, petroleum hydrocarbon can indefinitely persist in environments [5]. Consequently, understanding the interactions of gene activities in petroleum degradation in an inter-specific, networked, and comprehensive framework is key for understanding the microbial degradation of petroleum.

Metatranscriptomics allows the investigation of gene transcription within natural samples, in addition to the transcription and regulation of genes under specific conditions and in the life cycles of a specific population, thereby providing a more comprehensive understanding of the degradation of petroleum hydrocarbons by microbial metabolic activities. For example, Kothari compared the cultivation of

Acinetobacter venetianus RAG-1 on dodecane, dodecanol, and sodium acetate, observing that three genes were transcribed that were involved in alkane oxidation—*alkMa, alkMb*, and *almA*. Among these, *alkMb* exhibited the highest differential expression and may be involved in dodecane oxidation. Further comparison of the strain grown on sodium acetate medium led to the identification of 1,074 differentially expressed genes, of which 622 up-regulated genes were involved in alkane catabolism and stress response to alkanes [6]. Moreover, Hong observed that *Achromobacter*.sp. HZ01 can degrade anthracene, phenanthrene, pyrene, and n-alkanes, using polycyclic aromatic hydrocarbons as the sole carbon source after petroleum treatment of strain HZ01 for 16 h. In addition, a total of 742 differentially expressed genes were identified from strain HZ01 by transcriptomic analysis, with most down-regulated genes being related to cell motility, sugar metabolism, and ribosomal proteins, while genes involved in fatty acid metabolic pathways, some monooxygenases, and dehydrogenases were up-regulated, and TCA cycle genes were inactive [7]. Johanne Aubé compared a contaminated mat exposed to chronic petroleum contamination and a reference mat by using metagenomic and metatranscriptomic approaches. ABC transporters, two-component systems, and type IV secretion system-related genes were overabundant in the contaminated mats. Xenobiotic degradation metabolism was lesser in the metagenomes of both mats, and only the expression of genes involved in polycyclic aromatic hydrocarbon degradation was higher in the contaminated mat [8]. Thus, most previous studies have primarily focused on types of oil-degrading bacteria and their associated genes, while investigations have been lacking regarding the comprehensive regulation of marine oil hydrocarbon-degrading bacteria under specific environmental conditions (e.g., those associated with offshore drilling platforms). Consequently, this study evaluated the metabolic pathways and gene regulation of natural marine bacterial communities involved in the degradation of petroleum hydrocarbons. In particular, we systematically evaluated community structures, degradation pathways, and metabolic gene networks involved in petroleum hydrocarbon metabolism in near offshore drilling platform waters. The overall goal of the study was to provide a theoretical foundation for the microbial treatment of oil-spill accidents in offshore drilling platforms.

Materials And Methods

Experimental Materials and Sampling

Seawater samples were collected near an oil drilling platform located at 38°26’31.7” N, 118°24’45.2” W. Samples were divided into 13 equal portions, each of which comprised 50 L. For 12 of them, different culture conditions comprising high- and low-nutrient conditions, different aeration conditions, and conditions with or without oil were used to evaluate differences in gene transcription among treatments; the rest one was set as control (named as ORI group; the condition was kept as same as of the sampled seawater around oil drilling platform). Different ventilation conditions: Every day in the morning and evening, the 50 L seawater of barrel of each different aeration group was ventilated for half an hour with a steel cylinder filled with CO_2, O_2, or air. All flow rates are controlled at 5 mg L^{-1}. Detailed cultivation parameters are described in Table 1.

On the 1st, 5th, 15th, and 20th day of such culture, the bacteria in the seawater were filtered with a glass sand filter device to a 0.45μm and then a 0.22μm filter membrane, respectively. Each filter membrane was enriched with bacteria from 1000ml of seawater. The filter membrane, after bacterial enrichment, was divided into different 50ml centrifuge tubes according to different samples, marked, and stored in a refrigerator at -80℃. Gene transcription was evaluated by extracting RNA samples of treatment cultures on the 20th day of cultivation.

Experimental Methods

Fluorescence in Situ Hybridization (Fish) of Petroleum-Degrading Bacteria

Phosphorus absorption in *Alcanivorax borkumensis* is regulated by the high-affinity ABC transporter system that is composed of *phoU-pstBACS* and *phoBR* gene expression products through the Pit transport system in nutrient-rich environments (> 20 mM Pi). The *znuA* gene of *Alcanivorax borkumensis* is a periplasmic Zn^{2+} binding protein that is related to the high-affinity ATP-binding ZnuABC transport protein from *E. coli* [9]. In addition, *phoB* encodes positive regulators of the *E. coli* phosphor-regulator (including *phoA*, *phoS*, *phoE*, and *ugpAB*) [10]. Based on these previous studies, the following gene probes were used to evaluate gene transcription in the culture communities: *znuA*, *phoB*, *nqrf*, *rubb*, *znub*, *moda*, *gltx*, and *ecta*. The DNA of petroleum-degrading bacteria and performed primer verification were extracted. FISH was given on petroleum-degrading bacteria, and then used the American BD C6 flow cytometer (American BD Co., Tianjin Municipality, China) for detection.

Metatranscriptomic Analyses

RNA libraries were subjected to fragment screening prior to establishing the final RNA library. A quality-controlled library was then sequenced on the Illumina Hiseq high-throughput sequencing platform, and the raw data obtained from sequencing was used for subsequent transcriptomic analysis. Raw data was quality filtered to obtain clean data for evaluating taxonomic and functional differences between samples. The assembled sequencing data is available in the IMG/JGI (Integrated Microbial Genomes & Microbiomes, DOE's Joint Genome Institute, USA) database (GOLD Analysis Project IDs are, ORI: Ga0439915, OOL: Ga0439914, OOH: Ga0439913, ONL: Ga0439912, ONH: Ga0439911, COL: Ga0439910, COH: Ga0439909, CNL: Ga0439908, CNH: Ga0439504, AOL: Ga0439503, AOH: Ga0439502, ANL: Ga0439501, ANH: Ga0439470). The abbreviations mean specific transcriptomes from certain conditions: ORI, marine bacteria, directly from seawater, origin; OOL, marine bacteria, cultured with oxygen, oil(petroleum), and low nutrient content; OOH, oxygen, oil(petroleum), and high nutrient content; ONL, oxygen, no oil(petroleum), and low nutrient content; ONH, oxygen, no oil(petroleum), and high nutrient content; COL, carbon dioxide, oil(petroleum), and low nutrient content; COH, carbon dioxide, oil(petroleum), and high nutrient content; CNL, carbon dioxide, no oil(petroleum), and low nutrient content; CNH, carbon dioxide, no oil(petroleum), and high nutrient content; AOL, air, oil(petroleum), and low nutrient content; AOH, air, oil(petroleum), and high nutrient content; ANL, air, no oil(petroleum), and low nutrient content; ANH, air, no oil(petroleum), and high nutrient content.

BLAST (The Basic Local Alignment Search Tool) alignment (e value threshold of ≤ 1e-5 for positive hits) of the quality filtered data against the NCBI non-redundant (NR) protein database was conducted. The lowest common ancestor (LCA) classification algorithm implemented in MEGAN (Metagenome Analyser) [11] was used to assign taxonomic classifications based on alignments, since each sequence might have multiple alignment results. Specifically, the taxonomic classification based on the first branch served as the species annotation for the sequence in question. Relative abundances of the ten most abundant classes are shown in the results, with the largest relative abundances in each sample shown and the remaining taxa being grouped as “Others”.

Functional annotation of the quality filtered data was conducted using BLAST alignment of protein sequences against the assembled transcriptomic and protein annotation databases. Since multiple results could arise from each sequence alignment, the alignment results of each sequence were screened by calculating the alignment coverage ratio of each gene based on the reference and query lengths (i.e., the BLAST coverage ratio; BCR) to ensure that the BCR of the reference and query in each alignment exceeded 40%. The corresponding functional annotation information was then compiled from the databases.

Analysis of Metabolic Pathways

Digital gene expression (DGE) profiling was used to compare the expression differences between the transcriptomic responses of this study’s communities against that of transcriptome directly from marine environment. Metabolic pathway enrichment analysis based on KEGG pathways was then conducted in Pathview (a package in R) to investigate differences in metabolic pathway representation of differentially expressed genes under different conditions, in addition to identifying potential regulatory mechanisms of functional genes.

Results

Changes in Fluorescence Intensity of Petroleum-Degrading Bacteria under Different Culture Conditions

The fluorescence intensities of cultures under high- and low-nutrient conditions with and without oil amendment are shown in Figs. 1 and 2, respectively. In the presence of oil and oxygen, the genes 3 (*znuA*), 7 (*gltX*), and 8 (*ectA*) exhibited higher fluorescence intensity on the 10th day of culture under high-nutrient conditions than under low-nutrient conditions. In conditions with oil and carbon dioxide supplementation, the fluorescence intensity of gene 3 (*znuA*) was higher under high-nutrient conditions than under low-nutrient conditions on the 15th day of culture. When supplemented with oil and oxygen, the fluorescence intensity of gene 6 (*modA*) was higher under high-nutrient conditions than under low-nutrient conditions on the 20th day of culture. In non-oil amended, air-treated conditions, the fluorescence intensity of gene 2 (*phoB*) was higher under high-nutrient conditions than under low-nutrient conditions on the 15th day of culture. The non-oil amended and oxygen-treated condition cultures exhibited a higher fluorescence

intensity of gene 2 (*phoB*) under high-nutrient conditions than under low-nutrient conditions on the 10th day of culture. In addition, the non-oil amended and oxygen-treated condition cultures exhibited a higher fluorescence intensity of gene 6 (*modA*) on the 20th day of culture under high-nutrient conditions than under low-nutrient conditions.

The Metabolic Pathways of Marine Microbial Communities under Different Culture Conditions

Taxonomic Composition of Enrichment Cultures

The abundances of the ten most abundant organisms significantly increased in comparison with the original seawater sample community composition (Fig. 3). In particular, the ten most abundant organisms (at the class level) were: γ-Proteobacteria, Saccharomyces, α-Proteobacteria, Flavobacteria, Actinomycetes, ε-Proteobacteria, δ-Proteobacteria, β-Proteobacteria, Bacteroides, and Eurotium.

Variation in Functional Gene Composition Within Metabolic Pathways under Different Culture Conditions

The logarithmic ratios of the 20 most up-regulated (Table 2) and 20 most down-regulated (Table 3) differentially expressed genes within metabolic pathways under all conditions were specifically evaluated. The three most up-regulated protein encoding genes among all culture conditionsencoded 1) heat shock 70 kda proteins under COL vs ORI conditions, 2) heat shock 70 kda proteins under COL vs AOL conditions, and 3) superoxide dismutases within the Fe-Mn family under CNL vs ANL conditions. The three most down-regulated functional genes among all culture conditions were genes encoding 1) glutathione peroxidases under OOL vs AOL conditions, 2) elongation factor 1α-like proteins under CNL vs ANL conditions, and 3) GMP synthetases (glutamine hydrolysis) under CNH vs ANH conditions.

The Number of Metabolic Pathways under Different Culture Conditions

A total of 1,066 metabolic pathway maps were obtained under when comparing culture conditions (Table 4). The four culture condition comparisons of CNL vs CNH, CNH vs ANH, COH vs CNH, and CNH vs ORI exhibited the most pathways mapped. In addition, the ANL vs ANH and ONH vs ANH comparisons also exhibited numerous metabolic pathways.

Analysis of Functional Gene Metabolic Pathway Transcription under Different Culture Conditions

Different culture conditions with clearly different gene transcription profiles in metabolic pathways were selected for further evaluation. Comparisons between low- and high-nutrient conditions under air-treated and non-oil amended conditions (ANL vs ANH) are shown in Figs. 4 and 5, respectively. Glutamate decarboxylase (K01580), γ-glutamyl transpeptidase (K00681), and glutamate dehydrogenase (K00260) encoding genes were down-regulated in the taurine and hypotaurine metabolic regulation pathways (Fig. 4). Further, genes encoding inositol-1-phosphate synthase (K01858), phosphatidylinositol 4-kinase A (K00888), 1-phosphatidylinositol-3-phosphate 5-kinase (K00921), malonate-semialdehyde dehydrogenase (K00140) and triose phosphate isomerase (K01803) were down-regulated within the inositol phosphate metabolic pathway (Fig. 5).

Gene transcriptionn differences between carbon dioxide-treated and air-treated cultures under non-oil amended and high-nutrient conditions (CNH vs ANH) are shown in Fig. 6. Genes encoding galactokinase (K00849), hexokinase (K00844), and 6-phosphofructokinase 1 (K00850) were up-regulated in the galactose metabolic pathway. In contrast, genes encoding UTP-glucose-1-phosphate uridylyltransferase (K00963), glucose 4-epimerase (K01784), glutathione phosphate (K01835), maltose amylase (K12047), and other genes were down-regulated in the galactose metabolic pathway.

The gene transcription profile comparisons between oxygen-treated and air-treated cultures under non-oil amended and high-nutrient conditions (ONH vs ANH) are shown in Figs. 7 and 8, respectively. Genes encoding glucose 4-epimerase (K01784), glutathione phosphate (K01835), and maltose amylase (K12047) were up-regulated in the galactose metabolic pathway (Fig. 7). In addition, genes encoding glutamate decarboxylase (K01580) and γ-glutamyl transpeptidase (K00681) were down-regulated in the taurine and hypotaurine metabolic pathways (Fig. 8). In contrast, genes encoding proteins like cysteine dioxygenase (K00456) and glutamate dehydrogenase (K00260) were up-regulated in the taurine and hypotaurine metabolic pathway.

Comparisons between carbon dioxide-treated and oxygen-treated conditions under oil amended and high-nutrient conditions (COH vs OOH) are shown in Fig. 9. Genes encoding inositol-1-phosphate synthase (K01858) and phosphatidylinositol 4-kinase A (K00888) were up-regulated in the inositol phosphate metabolic pathway, while genes encoding malonate-semialdehyde dehydrogenase (K00140) and triose phosphate isomerase (K01803) were down-regulated in the inositol phosphate metabolic pathway.

Comparisons between the oil amended and non-oil amended conditions with carbon dioxide-treatment and high-nutrient conditions (COH vs CNH) are shown in Figs. 10 and 11. Genes encoding proteins, including sorbose reductase (K17742) and triose phosphate isomerase (K01803), were up-regulated in the fructose and mannose metabolic pathways (Fig. 10). In contrast, genes encoding hexokinase (K00844), mannose-1-phosphate guanylyltransferase (K00966), mannose-6-phosphate isomerase (K01809), 6-phosphate fructose-2-kinase (K00900), 6-phosphate fructokinase 1 (K00850), fructose-bisphosphate aldolase (K01623), dihydroxyacetone kinase (K00863), and 6-bisphosphatase I (K03841) were down-regulated in the fructose and mannose metabolic pathways. Genes encoding inositol-1-phosphate synthase (K01858), phosphatidylinositol 4-kinase A (K00888), 1-phosphatidylinositol-4-phosphate 5-

kinase (K00889), phosphatidylinositol alcohol 3-kinase (K00914), 1-phosphatidylinositol-3-phosphate 5-kinase (K00921), inositol oxygenase (K00469), malonate-semialdehyde dehydrogenase (K00140), and other genes were down-regulated in the inositol phosphate metabolic pathway (Fig. 11). In contrast, the triose phosphate isomerase (K01803) gene was up-regulated in the inositol phosphate metabolic pathway.

Discussion

Analysis of Optimal Culture Conditions

The optimal or sub-optimal nature of culture conditions can significantly effect gene expression and subsequent hybridization patterns [12]. Consequently, we compared changes in the fluorescence intensities of petroleum-degrading bacteria based on the hybridization with various probes under 12 culture conditions. The fluorescence intensities of cells under oxygen-treated conditions were the highest, indicating that oxygen-treatment conditions provided the most favorable culture environment for aerobic bacteria and therefore greater gene transcription hybridization. In addition, high-nutrient conditions provide adequate nutrient levels for cell growth, leading to greater levels of genes being expressed under high-nutrient conditions than in low-nutrient conditions.

Metabolic Pathway Analysis

Analysis of Pathways Differentially Expressed under ANL vs ANH Conditions

The metabolism of taurine and hypotaurine is primarily involved in the synthesis of taurine, hypotaurine, and their derivatives. Taurine and hypotaurine are antioxidants that protect cells from toxic oxidants [13]. Glutamate decarboxylase (K01580) catalyzes the transformation of 3-sulfinyl-L-alanine to hypotaurine, but also catalyzes the transformation of L-cysteine to taurine (Fig. 4) [14]. Thus, decreased nutrient concentrations will inhibit the activity of glutamate decarboxylase, resulting in less hypotaurine and taurine production. γ-glutamyl transpeptidase (K00681) catalyzes the transfer of γ-glutamyl to other amino acids and peptides, while also catalyzing the formation of 5-glutamyl-taurine from taurine within this metabolic pathway [15]. Decreased nutrient concentrations inhibited the activity of γ-glutamyl transpeptidase, likely leading to decreased end products. Glutamate dehydrogenase (K00260) catalyzes the reversible conversion of 2-oxoglutarate and L-glutamate [16] and decreased nutrient concentrations inhibited the activity of glutamate dehydrogenase when treated with air.

Metabolism of inositol phosphate is used to synthesize inositol phosphate (Fig. 5) that can be used as a second messenger for a variety of extracellular signals [17]. Inositol-1-phosphate synthase (K01858) catalyzes the conversion of D-glucose-6-phosphate to 1L-inositol-1-phosphate, with an intermediate product of 1D-inositol-3-phosphate [18]. When nutrient concentrations were lowered, the activity of

inositol-1-phosphate synthase was inhibited, thereby reducing 1D-inositol-3-phosphate concentrations. Phosphatidylinositol 4-kinase A (K00888) catalyzes the conversion of PtdIns into 4-phosphate PtdIns [19] and decreased nutrient concentrations inhibited the activity of phosphatidylinositol 4-kinase A, therefore likely reducing product levels. 1-phosphatidylinositol-3-phosphate 5-kinase (K00921) catalyzes the conversion of 3-phosphate PtdIns into PtdIns-3, 5-P(2) [20], and lowered nutrient concentrations inhibited 1-phosphatidylinositol-3-phosphate 5-kinase activity, thereby likely resulting in decreased product levels. Malonate-semialdehyde dehydrogenase (K00140) catalyzes the oxidation of malonate semialdehyde (MSA) to acetyl-CoA [21]. The lower nutrient concentration treatment led to the inhibition of malonate-semialdehyde dehydrogenase activity. Triose phosphate isomerase (K01803) regulates the rapid balancing of dihydroxyacetone phosphate and glyceraldehyde-3-phosphate produced by aldolase during glycolysis [22], and decreased nutrient concentrations led to inhibition of its activity.

In summary, decreased nutrient concentrations inhibited the metabolic pathways of taurine and hypotaurine, thereby likely reducing the production of taurine and hypotaurine, and potentially enhancing the impact of harmful oxidants on cells. At the same time, these decrease also inhibit the metabolism of inositol phosphate and reduce the synthesis of inositol phosphate, potentially leading to losses of extracellular signaling and inhibiting cell growth and metabolism. Consequently, these results indicate that bacteria require sufficient nutrient levels to secure their own growth and reproduction requirements.

Analysis Of Metabolic Pathways Differentially Expressed under CNH vs ANH Conditions

Galactose metabolism involves the conversion of polysaccharides into monosaccharides like galactose and glucose. Galactose also exhibits a strong inhibitory effect on cell growth [23]. Galactokinase (K00849) catalyzes the conversion of α-D-galactose into galactose 1-phosphate (Fig. 6) [24]. The carbon dioxide-treated condition in the CNH and ANH treatments led to the enhancement of galactokinase activity, leading to increased levels of galactose 1-phosphate. UTP-glucose-1-phosphate uridylyltransferase (K00963) catalyzes the synthesis of UDP-glucose from glucose-1-phosphate and UTP [25]. However, in the carbon dioxide vs air treatment with high nutrients, the carbon dioxide-treatment conditions reduced the activity of the transferase. Glucose 4-epimerase (K01784) catalyzes the mutual conversion of UDP-galactose and UDP-glucose [26]. Compared with air-treated conditions, carbon dioxide treatment inhibited the activity of the epimerase and likely reduced the conversion efficiency of the above reaction. In addition, glutathione phosphate (K01835) is a necessary enzyme for the mutual conversion of glucose 1-phosphate and glucose 6-phosphate [27]. Likewise, carbon dioxide treatment inhibited the activity of glutathione phosphate, thereby likely reducing the transformation efficiency of this reaction as well. Hexokinase (K00844) phosphorylates glucose, catalyzing the conversion of glucose to glucose 6-phosphate [28]. The carbon dioxide treatment increased the activity of hexokinase compared to the air-treated conditions, thereby increasing the efficiency of glucose phosphorylation. Maltose amylase (K12047) converts glucan derived from starch decomposition into glucose [29]. When comparing the CNH and ANH conditions, the carbon dioxide-treated conditions inhibited the activity of maltogenic amylase, thereby likely leading to reduced levels of glucose production. 6-phosphofructokinase 1 (K00850)

catalyzes the conversion of 6-phosphate fructose to 1,6-diphosphate [30]. Carbon dioxide treatment also enhanced the activity of 6-phosphofructokinase 1 in the CNH vs ANH comparisons, likely leading to increased conversion efficiency of the above product.

Overall, changes of enzyme activity in the CNH vs ANH conditions led to increased galactose content, thereby inhibiting cell growth, with bacteria likely growing better in air-treated conditions.

Analysis of Metabolic Pathways Differentially Expressed under ONH vs ANH Conditions

Galactose metabolism converts polysaccharides into monosaccharides like galactose and glucose (Fig. 7). Glucose 4-epimerase (K01784) catalyzes the mutual conversion of UDP-galactose and UDP-glucose [26]. Oxygen treatment enhanced the isomerase activity compared to the air-treated conditions and thus, likely the overall conversion efficiency of this reaction. Glutathione phosphate (K01835) is an enzyme necessary for the mutual conversion of glucose 1-phosphate and glucose 6-phosphate [27]. The oxygen-treatment in the ONH vs ANH treatment apparently enhanced the activity of glutathione phosphate, which would lead to increased transformation efficiency of the above reaction. Maltose amylase (K12047) converts glucan derived from starch decomposition into glucose [29], and oxygen treatment enhances the activity of maltogenic amylase and thus, the likely production of glucose when comparing the ONH and ANH conditions.

Cysteine dioxygenase (K00456) sulfonates and oxidizes cysteine to cysteine sulfinic acid (Fig. 8) [31] and catalyzes the transformation of cysteine to 3-sulfinyl-L-alanine in this metabolic pathway. Oxygen addition increased the expression of cysteine dioxygenase compared with the air-ventilated condition. Glutamate decarboxylase (K01580) catalyzes the transformation of 3-sulfinyl-L-alanine to hypotaurine, but also catalyzes the transformation of L-cysteine to taurine [14]. Oxygen inhibited the activity of glutamate decarboxylase in the ONH vs ANH comparison, which would result in a decrease in the products hypotaurine and taurine. γ-glutamyl transpeptidase (K00681) can catalyze the transfer of γ-glutamyl to other amino acids and peptides, while catalyzing the formation of 5-glutamyl-taurine from taurine via this metabolic pathway [15]. Oxygen also inhibited the activity of γ-glutamyl transpeptidase, which would result in decreased reaction products. Glutamate dehydrogenase (K00260) can catalyze the reversible conversion of 2-oxoglutarate and L-glutamate [16] and its activity was up-regulated by oxygen treatment compared with the air-ventilated condition.

In conclusion, oxygen-treatment conditions compared to air-treatment conditions promote the metabolism of galactose, accelerate polysaccharide degradation efficiency and provide additional nutrients for bacterial growth. Thus, bacteria would exhibit better survival under oxygen treatment conditions. At the same time, oxygen will reduce the production of taurine and hypotaurine compared with air-treatment conditions. Thus, taurine and hypotaurine content will increase under air-treated conditions, potentially due to the presence of harmful oxidants present in air relative to exposure to only oxygen. Increasing taurine and hypotaurine content will inhibit the effect of harmful oxidants on cells.

Analysis of Metabolic Pathways Differentially Expressed under COH vs OOH Conditions

Inositol-1-phosphate synthase (K01858) catalyzes the conversion of D-glucose-6-phosphate into 1L-inositol-1-phosphate, forming the intermediate product of 1D-inositol-3-phosphate (Fig. 9) [18]. Compared with oxygen-treated condition, carbon dioxide treatment enhances the activity of inositol-1-phosphate synthase, which in turn increases 1D-inositol-3-phosphate levels. Phosphatidylinositol 4-kinase A (K00888) catalyzes the conversion of PtdIns to 4-phosphate PtdIns [19]. The COH treatment enhanced the activity of phosphatidylinositol 4-kinase A compared to the OOH condition and would lead to increased product levels. Malonate-semialdehyde dehydrogenase (K00140) catalyzes the oxidation of malonate semialdehyde (MSA) to acetyl-CoA [21]. Compared with oxygen-treated conditions, carbon dioxide inhibited the activity of malonate-semialdehyde dehydrogenase. Triose phosphate isomerase (K01803) regulates the rapid balancing of dihydroxyacetone phosphate and glyceraldehyde-3-phosphate that are produced by aldolase in the glycolysis process [22]. Compared with the OOH condition, COH conditions will inhibit the activity of triose phosphate isomerase.

In conclusion, the COH condition increased the synthesis capacity for inositol phosphate compared to OOH conditions, which resulted in increased extracellular signal transmission. Thus, carbon dioxide treatments would lead to unfavorable factors against bacterial growth and reproduction, with cells needing to transmit increasing levels of signals to regulate growth and metabolism.

Analysis of Metabolic Pathways Differentially Expressed under COH vs CNH Conditions

A series of enzymes are needed to transform monosaccharides like L-sorbose and D-allose into fructose, mannose, and glucose. Sorbose reductase (K17742) converts L-sorbose into D-sorbitol (Fig. 10) [32]. When oil was added as the carbon source, sorbose reductase activity is enhanced and the conversion rate likely increases. Hexokinase (K00844) phosphorylates glucose [28] and catalyzes fructose and mannose conversion to fructose 6-phosphate and mannose 6-phosphate, respectively. When oil was added as the carbon source, hexokinase activity was inhibited. Mannose-1-phosphate guanylyltransferase (K00966) catalyzes the reaction of mannose-1-phosphate and GTP to produce GDP mannose [33]. When oil was added as the carbon source, transferase activity was inhibited. Mannose-6-phosphate isomerase (K01809) catalyzes the mutual conversion of mannose 6-phosphate (Man-6-P) and fructose 6-phosphate (Fru-6-P) [34], and adding oil as the carbon source inhibited the activity of the isomerase, thereby restricting this mutual conversion activity. Fructose 2,6-diphosphate is a signal molecule that controls glycolysis, and 6-phosphate fructose-2-kinase (K00900) catalyzes the synthesis of fructose 6-phosphate into fructose 2,6-diphosphate [35]. When oil was added as the carbon source, 6-phosphofructose-2-kinase activity was inhibited. Fructose-1,6-bisphosphatase I (K03841) catalyzes the conversion of fructose 1,6-diphosphate into fructose 6-phosphate [36]. When oil was added as the carbon source, the activity of fructose-1,6-bisphosphatase I was inhibited and the conversion to fructose 6-phosphate would have thus been reduced. 6-phosphofructokinase 1 (K00850) catalyzes the conversion of 6-phosphate fructose to

1,6-diphosphate [30], but adding oil as the carbon source inhibited the activity of 6-phosphofructokinase 1. Fructose-bisphosphate aldolase (K01623) catalyzes the condensation of glucose-3-phosphate and dihydroxyacetone phosphate to form fructose 1,6-diphosphate [37]. Under the oil addition treatment, the activity of fructose-bisphosphate aldolase was inhibited, resulting in a likely decrease of fructose 1,6-diphosphate products. Triose phosphate isomerase (K01803) regulates the rapid balancing of dihydroxyacetone phosphate and glyceraldehyde-3-phosphate produced by aldolase during glycolysis [22]. When oil was added as the carbon source, the activity of triose phosphate isomerase increased and the mutual conversion rate likely increased. Dihydroxyacetone kinase (K00863) phosphorylates fructose-derived glyceraldehyde to produce glyceraldehyde-3-phosphate [38]. When oil was added as the carbon source, the activity of dihydroxyacetone kinase was inhibited, likely leading to a decrease in product formation.

Inositol-1-phosphate synthase (K01858) catalyzes the conversion of D-glucose-6-phosphate to 1L-inositol-1-phosphate (Fig. 11), with the intermediate product being 1D-inositol-3-phosphate [18]. When oil was added as the carbon source, inositol-1-phosphate synthase activity was inhibited, thereby reducing the amount of 1D-inositol-3-phosphate that was produced. Phosphatidylinositol 4-kinase A (K00888) catalyzes the conversion of phosphatidylinositol (PtdIns) into 4-phosphate PtdIns [19]. Upon oil addition treatment, inhibited activity of phosphatidylinositol 4-kinase A would result in decreased product levels. 1-phosphatidylinositol-4-phosphate 5-kinase (K00889) catalyzes the synthesis of 4-phosphate PtdIns to 4,5-bisphosphate PtdIns [39], and decreased nutrient concentrations inhibited the activity of 1-phosphatidylinositol-4-phosphate 5-kinase. Phosphatidylinositol 3-kinase (K00914) catalyzes the transformation of PtdIns to produce 3-phosphate PtdIns [40], while the addition of oil as a carbon source inhibited the activity of phosphatidylinositol 3-kinase, thereby likely decreasing the levels of the product PtdIns. 1-phosphatidylinositol-3-phosphate 5-kinase (K00921) catalyzes the conversion of 3-phosphate PtdIns to PtdIns-3,5-P(2) [20], and when oil was added as the carbon source, the activity of 1-phosphatidylinositol-3-phosphate 5-kinase was inhibited, likely resulting in a decrease in its product. Malonate-semialdehyde dehydrogenase (K00140) catalyzes the oxidation of malonate semialdehyde (MSA) to acetyl-CoA [21]. When oil was added as the carbon source, the activity of malonate-semialdehyde dehydrogenase was inhibited. Triose phosphate isomerase (K01803) regulates the rapid balancing of dihydroxyacetone phosphate and glyceraldehyde-3-phosphate that are produced by aldolase during glycolysis [22]. When oil was added as a carbon source, the activity of triose phosphate isomerase was enhanced. Inositol oxygenase (K00469) is the only mechanism to catabolize inositol, wherein it catalyzes the cleavage of the inositol ring and transfers an oxygen atom to it [41]. This metabolism catalyzes the decomposition of inositol into glucuronate and the addition of oil as a carbon source inhibited the activity of inositol oxygenase, thereby likely reducing the decomposition efficiency of inositol.

Overall, the addition of oil as a carbon source led to the inhibition of fructose and mannose metabolism and the concomitant decrease in fructose and mannose production. Thus, the ability of populations to consume sugar for survival will be lessened under such conditions, and oil will instead be degraded for energy conservation. Concomitantly, the addition of oil as the carbon source will inhibit the metabolism of

inositol phosphate and reduce its synthesis, leading to the loss of extracellular signaling, thereby inhibiting cell growth along with metabolism and other activities. Thus, the addition of oil results in counterproductive effects on the growth and reproduction of bacteria.

Conclusions

This study investigated the transcriptomic responses of seawater microbial communities that were collected from near a drilling platform in Bohai Bay in response to varying enrichment incubations. We specifically evaluated the transcription of enzyme-encoding genes and their related metabolic pathways that were associated with hydrocarbon metabolism and energy conservation. The enrichment culture cells and their metabolic activities exhibited differential adaptations to the enrichment conditions and exhibited different responses to aerobic and anaerobic culture conditions. Metabolic pathway transcription and functional gene analyses suggested that high-nutrient, oil-free, and aerobic culture conditions largely promoted the growth and reproduction of marine microbial populations. Understanding how these microorganisms may degrade hydrocarbons is an important focus for helping to remediate oil spill ecological problems. These results can help develop remediation protocols for oil spills.

Declarations

Acknowledgment

We thank LetPub (www.letpub.com) for its linguistic assistance and scientific consultation during the preparation of this manuscript.

Funding Information

The study was supported by Natural Science Foundation of Hebei Province, China (Grant No. D2020202004), National Natural Science Foundation of China Youth Project (Grant No. 31801948), National Natural Science Foundation of China (Grant No. 51474084 and Grant No. 21978065), Key R&D Projects in Hebei Province (Grant No. 19226505D), Tianjin Science and Technology Committee (No.18ZXRHSF00270).

Conflict of Interest Statement

The authors declare that they have no conflict of interest.

Declaration of Competing Interest

The authors declare that they have no known competing financial interests or personal relationships that could have appeared to influence the work reported in this paper.

References

1. Pawl T, Edward J (1991) Hydrocarbon contaminated soils and groundwater. Lewis Publishers INC, Lewis
2. Delille D, Basseres A, Dessommes A (1998) Effectiveness of bioremediation for oil-polluted Antarctic seawater. Polar Biology 19:237–241. https://doi.org/10.1007/s003000050240
3. Das N, Chandran P (2011) Microbial Degradation of Petroleum Hydrocarbon Contaminants: An Overview. Biotechnology Research International. https://doi.org/10.4061/2011/941810
4. Sekelsky, A.M., Shreve, G.S. (1999) Kinetic model of biosurfactant-enhanced hexadecane biodegradation by Pseudomonas aeruginosa. Biotechnology and bioengineering.63,401–409. https://doi.org/10.1002/(SICI)1097-0290(19990520)63:4<401::AID-BIT3>3.0.CO;2-S
5. Li L, Zhang L, Zhang Y (2001) Research overview of petroleum hydrocarbon-degrading bacteria. Microbiology China 28.5:89–92
6. Kothari A, Charrier M, Wu YW et al (2016) Transcriptomic analysis of the highly efficient oil-degrading bacterium Acinetobacter venetianus RAG-1 reveals genes important in dodecane uptake and utilization. FEMS Microbiol Lett 363(20):fnw224. https://doi.org/10.1093/femsle/fnw224
7. Hong Y, Deng M, Xu X et al (2016) Characterization of the transcriptome of Achromobacter sp. HZ01 with the outstanding hydrocarbon-degrading ability. Gene 584(2):185–194. https://doi.org/10.1016/j.gene.2016.02.032
8. Aubé J, Senin P, Bonin P et al (2020) Meta-omics Provides Insights into the Impact of Hydrocarbon Contamination on Microbial Mat Functioning. Microb Ecol 80:286–295. https://doi.org/10.1007/s00248-020-01493-x
9. Liliya A, Yatsunyk J, Allen,Easton,Lydia R, Kim,Stacy (2008) Structure and metal binding properties of ZnuA, a periplasmic zinc transporter from Escherichia coli. J Biol Inorg Chem 13:271–288. https://doi.org/10.1007/s00775-007-0320-0
10. Makino. K, Shinagawa H, Amemura M, Nakata A (1986) Nucleotide sequence of the phoB gene, the positive regulatory gene for the phosphate regulon of Escherichia coli K-12. J Journal of Molecular Biology 190:37–44. https://doi.org/10.1016/0022-2836(86)90073-2
11. Huson DH et al (2007) MEGAN analysis of metagenomic data. Genome Res 17(3):377–386
12. He Y, Chen C, Huang B (2018) The regulation of bacterial small non-coding RNA on gene expression under environmental stress. Journal of Molecular Diagnosis Therapy 10:125–131,144. https://doi.org/10.3969/j.issn.1674-6929.2018.02.011
13. L. D B (1990) Taurine and hypotaurine content of human leukocytes. Journal of leukocyte biology. 2. https://doi.org/10.1111/j.1365-2141.1990.tb07825.x
14. Weinstein CL, Griffith OWJMiE (1987) Cysteinesulfinate decarboxylase. Methods in Enzymology 143,404. https://doi.org/ 10.1016/0166–0934(87)90050-4
15. Toshihiro O, Hideyuki S, Kei W, Hidehiko K, F.J.P.o.t.N.A.o.S.o.t.U.S.o.A. Keiichi (2006) Crystal structures of γ-glutamyltranspeptidase from Escherichia coli, a key enzyme in glutathione metabolism, and its reaction intermediate. Proceedings of the National Academy of Sciences. 103 (17),6471–6476. https://doi.org/10.1073/pnas.0511020103

16. Srivastava HS, Singh RPJP (1987) Role and regulation of L -glutamate dehydrogenase activity in higher plants. 26,597–610
17. Mishra J, U.S.J.B.J., Bhalla (2002) Simulations of Inositol Phosphate Metabolism and Its Interaction with InsP-Mediated Calcium Release. 83,1298–1316. https://doi.org/10.1016/S0006-3495(02)73901-5
18. Majumder AL, Johnson MD, A.J.B.B.A. S, Henry (1997) 1L - myo -inositol-1-phosphate synthase. Biochim Biophys Acta 1348:245–256
19. Balla A, Balla TJTiCB (2006) Phosphatidylinositol 4-kinases: old enzymes with emerging functions. Trends in cell biology 16:351–361. https://doi.org/10.1016/j.tcb.2006.05.003
20. Diego S, Ikonomov OC, Robert D, SJJ.o.BC Assia (2002) Phosphatidylinositol 5-phosphate biosynthesis is linked to PIKfyve and is involved in osmotic response pathway in mammalian cells. Journal of Biological Chemistry Journal of Biological Chemistry 277:47276–47284. https://doi.org/10.1074/jbc.M207576200
21. Claire SC, Guy BJBJ (2006) Mechanistic characterization of the MSDH (methylmalonate semialdehyde dehydrogenase) from Bacillus subtilis. Biochemical Journal 395:107–115. https://doi.org/10.1042/BJ20051525
22. Ferene O, Judit O, Judit OJIL (2006) Triosephosphate isomerase deficiency: facts and doubts. IUBMB Life 58:703–715. https://doi.org/10.1080/15216540601115960
23. Aki K (2007) Different effects of galactose and mannose on cell proliferation and intracellular soluble sugar levels in Vigna angularis suspension cultures. Journal of plant research. 6. https://doi.org/10.1007/s10265-007-0117-9
24. Holden HM, Thoden J, Timson D, Reece R (2004) Galactokinase: Structure, function and role in type II galactosemia. Cellular and Molecular Life Sciences CMLS. https://doi.org/10.1007/s00018-004-4160-6
25. Thoden JB, Holden HMJPS (2010) Active site geometry of glucose-1-phosphate uridylyltransferase. Protein Sci 16:1379–1388. https://doi.org/10.1110/ps.072864707
26. Thoden JB, Frey PA, Holden HM (1996) Molecular structure of the NADH/UDP-glucose abortive complex of UDP-galactose 4-epimerase from Escherichia coli: implications for the catalytic mechanism. Biochemistry 35:5137–5144. https://doi.org/10.1021/bi9601114
27. Lu M., Kleckner N (1994) Molecular cloning and characterization of the pgm gene encoding phosphoglucomutase of Escherichia coli. J Bacteriol 176:5847–5851. https://doi.org/10.1111/j.1365-2672.1994.tb03084.x
28. John W E (2003) Isozymes of mammalian hexokinase: structure, subcellular localization and metabolic function. The Journal of experimental biology Pt 12. https://doi.org/10.1242/jeb.00241
29. Maricela DS, Roberto QC, Avery SE, Chacko SK, Li-Ke Y, Amy Hui-Mei L, Zi-Hua A, Hamaker BR, Nichols BL (2013) Maltase-glucoamylase modulates gluconeogenesis and sucrase-isomaltase dominates starch digestion glucogenesis. Journal of Pediatric Gastroenterology Nutrition 57:704–712. https://doi.org/10.1097/MPG.0b013e3182a27438

30. Currie MA, Merino F, Skarina T, Wong AHY, Singer A, Brown G, Savchenko A, Caniuguir A, Guixé V, A.F.J.J.o.BYakunin C (2009) ADP-dependent 6-Phosphofructokinase from Pyrococcus horikoshii OT3. J Biol Chem.284,22664–22671. https://doi.org/10.1074/jbc.M109.012401
31. Dominy JE, Simmons CR, Andrew KP, Gehring AM, Stipanuk MH (2006) Identification and characterization of bacterial cysteine dioxygenases: a new route of cysteine degradation for eubacteria. Journal of Bacteriology 188:5561–5569. https://doi.org/10.1128/JB.00291-06
32. Greenberg JR, Price NP, Oliver RP, Fred S, Elena RJY (2010) Candida albicans SOU1 encodes a sorbose reductase required for L-sorbose utilization. Yeast 22:957–969. https://doi.org/10.1002/yea.1282
33. Diez MDA, Demonte A, Giacomelli J, Garay S, Rodrígues D, Hofmann B, Hecht HJ, Guerrero SA, A.A.J.A.o.MIglesias (2010) Functional characterization of GDP-mannose pyrophosphorylase from Leptospira interrogans serovar Copenhageni. Archives of Microbiology. 192,103. https://doi.org/10.1007/s00203-009-0534-3
34. Wenxia F, Xiaoying Y, Bin W, Hui Z, Haomiao O, Jia M, Cheng JJM (2009) Characterization of the Aspergillus fumigatus phosphomannose isomerase Pmi1 and its impact on cell wall synthesis and morphogenesis. Microbiology 155:3281–3293. https://doi.org/10.1099/mic.0.029975-0
35. Rider MH, Bertrand L, Vertommen D, Michels PA, Rousseau GG, Hue LJBJ (2004) 6-phosphofructo-2-kinase/fructose-2,6-bisphosphatase: head-to-head with a bifunctional enzyme that controls glycolysis. Biochemical Journal 381(Pt 3):561–579. https://doi.org/10.1042/BJ20040752
36. Naeem R, Hiroyuki I, Tamotsu K, Toshiaki F, Haruyuki A, I.J.J.o.B.C. Tadayuki (2002) A novel candidate for the true fructose-1,6-bisphosphatase in archaea. Journal of Biological Chemistry. 277, 30649–30655. https://doi.org/10.1074/jbc.M202868200
37. Lorentzen E, Siebers B, Hensel R, Pohl EJBST (2004) Structure, function and evolution of the Archaeal class I fructose-1,6-bisphosphate aldolase. Biochemical society transactions. 32,259. https://doi.org/10.1042/BST0320259
38. Joaquim Rui R (2014) Bifunctional homodimeric triokinase/FMN cyclase: contribution of protein domains to the activities of the human enzyme and molecular dynamics simulation of domain movements. Journal of biological chemistry.15. https://doi.org/10.1074/jbc.M113.525626
39. Xie Z, Chang SM, Pennypacker SD, Liao EY, DDJ.M.B.o.t.C. Bikle (2009) Phosphatidylinositol-4-phosphate 5-kinase 1alpha mediates extracellular calcium-induced keratinocyte differentiation. Molecular biology of the cell. 20,1695. https://doi.org/10.1091/mbc.E08-07-0756
40. Volinia S, Dhand,. R, Vanhaesebroeck B,., Macdougall LK, Stein,. R, Zvelebil MJ, Domin J,., Panaretou C, ., Waterfield MD (1995)) A human phosphatidylinositol 3-kinase complex related to the yeast Vps34p-Vps15p protein sorting system. Embo Journal 14:3339–3348. https://doi.org/10.1002/j.1460-2075.1995.tb07340.x
41. Arner RJ, Prabhu KS, Thompson JT, Hildenbrandt GR, Liken AD, Reddy CC (2002) Myo-inositol oxygenase: molecular cloning and expression of a unique enzyme that oxidizes myo-inositol and d-chiro-inositol. Biochemical Journal 360:313–320. https://doi.org/10.1042/bj3600313

Tables

Table 1

Setting of cultivation conditions for response of microbial communities near offshore drilling platforms to conditional changes

Sample codings	Sample description	Detailed cultivation parameters					
	Sample sources and processing, time point etc., condition types	Oil concentration	NO_3^- (mg/l)	PO_4^{3-} (mg/l)	NO_2^- (mg/l)	pH (CO_2 causes acidification)	Dissolved oxygen (mg/l)
COL	Marine bacteria, carbon dioxide, oil, low-nutrient culture	1%	13	182	0.03	6.13	2.2
COH	Marine bacteria, carbon dioxide, oil, high-nutrient culture	1%	1300	785	87	6.18	1.7
CNL	Marine bacteria, carbon dioxide, non-oil, low-nutrient culture	0%	7	15	0.06	6.59	3.6
CNH	Marine bacteria, carbon dioxide, non-oil, high-nutrient culture	0%	180	1300	179	6.43	1.3
OOL	Marine bacteria, oxygen, oil, low-nutrient culture	1%	11	9	0.04	7.15	7.1
OOH	Marine bacteria, oxygen, oil, high-nutrient culture	1%	800	1640	297	6.9	7.6

ONL	Marine bacteria, oxygen, non-oil, low-nutrient culture	0%	14	20	0.05	8.17	4.6
ONH	Marine bacteria, oxygen, non-oil, high-nutrient culture	0%	270	1155	237	6.96	6
AOL	Marine bacteria, air, oil, low-nutrient culture	1%	6	73	0.05	6.86	1.4
AOH	Marine bacteria, air, oil, high-nutrient culture	1%	750	2600	161	7.51	2.9
ANL	Marine bacteria, air, non-oil, low-nutrient culture	0%	5	37	0.06	8.02	3.8
ANH	Marine bacteria, air, non-oil, high-nutrient culture	0%	860	1300	253	7.06	3
ORI	Marine bacteria, directly collected from the seawater at drilling platform, original point	0%	0.0279	0.00021	0.0279	8.21	3.6

Table 2

The twenty most up-regulated genes in the transcriptomes of marine petroleum hydrocarbon-degrading bacterial populations under different enrichment conditions.

Rank	Treatment Comparison	Gene ID	KEGG Orthology ID	Annotation	log_2 Fold change
1	COL vs ORI	CNHc25501_g1	K09490	Heat shock 70 kDa protein 5	17.351
2	COL vs AOL	CNHc25501_g1	K09490	Heat shock 70 kDa protein 5	16.69
3	CNL vs ANL	CNLc46456_g2	K04564	Superoxide dismutase, Fe-Mn family	16.648
4	CNL vs ANL	CNLc46305_g2	K00111	Glycerol-3-phosphate dehydrogenase	16.066
5	ONL vs ORI	ONLc108377_g1	K13525	Transitional endoplasmic reticulum ATPase	15.879
6	COH vs ORI	ONHc38088_g7	K01803	Triosephosphate isomerase (TIM)	15.41
7	COL vs AOL	CNLc46973_g1	K14403	Cleavage and polyadenylation specificity factor subunit 3	15.325
8	COH vs ORI	OOHc45325_g1	K03231	Elongation factor 1-alpha	14.978
9	CNH vs ORI	CNHc25422_g5	K01868	Threonyl-tRNA synthetase	14.919
10	CNL vs ANL	CNLc47032_g1	K07513	Acetyl-CoA acyltransferase 1	14.89
11	CNL vs ANL	CNLc46097_g1	K14572	Midasin	14.856
12	CNL vs ANL	CNLc46329_g1	K00432	Glutathione peroxidase	14.697
13	COL vs OOL	COLc132630_g1	K11233	Osomolarity two-component system, Response regulator SSK1	14.638
14	COL vs AOL	COHc206826_g1	K04079	Molecular chaperone HtpG	14.572
15	OOL vs OOH	OOLc165459_g4	K08955	ATP-dependent metalloprotease	14.501
16	COL vs ORI	COHc206952_g2	K04079	Molecular chaperone HtpG	14.479
17	OOL vs OOH	COHc205626_g3	K14416	Elongation factor 1 α-like protein	14.414
18	OOL vs OOH	ONLc108377_g1	K13525	Transitional endoplasmic reticulum ATPase	14.413
19	OOL vs OOH	OOLc167494_g5	K14403	Cleavage and polyadenylation specificity factor subunit 3	14.373
20	COL vs ORI	COLc129759_g1	K10901	Bloom syndrome protein	14.299

Table 3

The twenty most down-regulated genes in the transcriptomes of marine petroleum hydrocarbon-degrading bacterial populations under different enrichment conditions.

Rank	Treatment Comparison	Gene ID	KEGG Orthology ID	Definition	log_2 Fold change
1	OOL vs AOL	AOLc124810_g1	K00432	Glutathione peroxidase	−17.446
2	CNL vs ANL	ANLc85495_g1	K14416	Elongation factor 1 alpha-like protein	−15.481
3	CNH vs ANH	OOHc45443_g1	K01951	GMP synthase (glutamine-hydrolysing)	−15.469
4	COH vs AOH	ANHc41385_g1	K14572	Midasin	−15.288
5	CNH vs ANH	ANHc42565_g1	K03781	Catalase	−15.278
6	COH vs CNH	ANHc40531_g1	K02145	V-type H+-transporting ATPase subunit A	−15.076
7	CNL vs ANL	ANLc86683_g1	K12818	ATP-dependent RNA helicase DHX8/PRP22	−14.911
8	CNL vs ANL	AOHc60780_g2	K00326	Cytochrome-b5 reductase	−14.879
9	CNL vs ANL	ANLc89125_g1	K01810	Glucose-6-phosphate isomerase	−14.795
10	COH vs CNH	CNHc11955_g1	K09468	Zinc finger protein MSN2/4	−14.721
11	CNL vs ANL	ANLc89286_g1	K08955	ATP-dependent metalloprotease	−14.646
12	COH vs CNH	ONHc35651_g1	K09580	Protein disulfide-isomerase A1	−14.411
13	CNH vs ANH	ANHc42678_g1	K03106	Signal recognition particle subunit SRP54	−14.36
14	COH vs AOH	AOHc61941_g4	K00966	Mannose-1-phosphate guanylyltransferase	−14.353
15	CNH vs ANH	AOLc124685_g1	K00762	Orotate phosphoribosyltransferase	−14.308
16	CNL vs ONL	ONLc108377_g1	K13525	Transitional endoplasmic reticulum ATPase	−14.291
17	CNH vs ANH	AOHc61110_g1	K08744	Cardiolipin synthase (CMP-forming)	−14.29
18	CNH vs ANH	ANHc38916_g1	K12818	ATP-dependent RNA helicase DHX8/PRP22	−14.252
19	COH vs CNH	ANHc40011_g1	K10967	Alpha 1,2-mannosyltransferase	−14.198
20	COH vs CNH	CNHc6836_g1	K03252	Translation initiation factor 3 subunit C	−14.184

Table 4

Number of metabolic pathways mapped to the transcriptomes from different conditions.

Treatment Comparison	Pathways	Treatment Comparison	Pathways
ANH vs ORI	36	COL vs AOL	29
ANL vs ANH	38	COL vs CNL	38
ANL vs ORI	32	COL vs COH	32
AOL vs ORI	32	COL vs OOL	30
CNH vs ANH	48	COL vs ORI	30
CNH vs ONH	36	ONH vs ANH	38
CNH vs ORI	45	ONH vs ORI	31
CNL vs ANL	39	ONL vs ANL	41
CNL vs CNH	50	ONL vs ORI	35
CNL vs ONL	35	OOH vs AOH	32
CNL vs ORI	35	OOH vs ORI	29
COH vs AOH	31	OOL vs AOL	35
COH vs CNH	45	OOL vs ONL	33
COH vs OOH	31	OOL vs OOH	32
COH vs ORI	35	OOL vs ORI	33

Figures

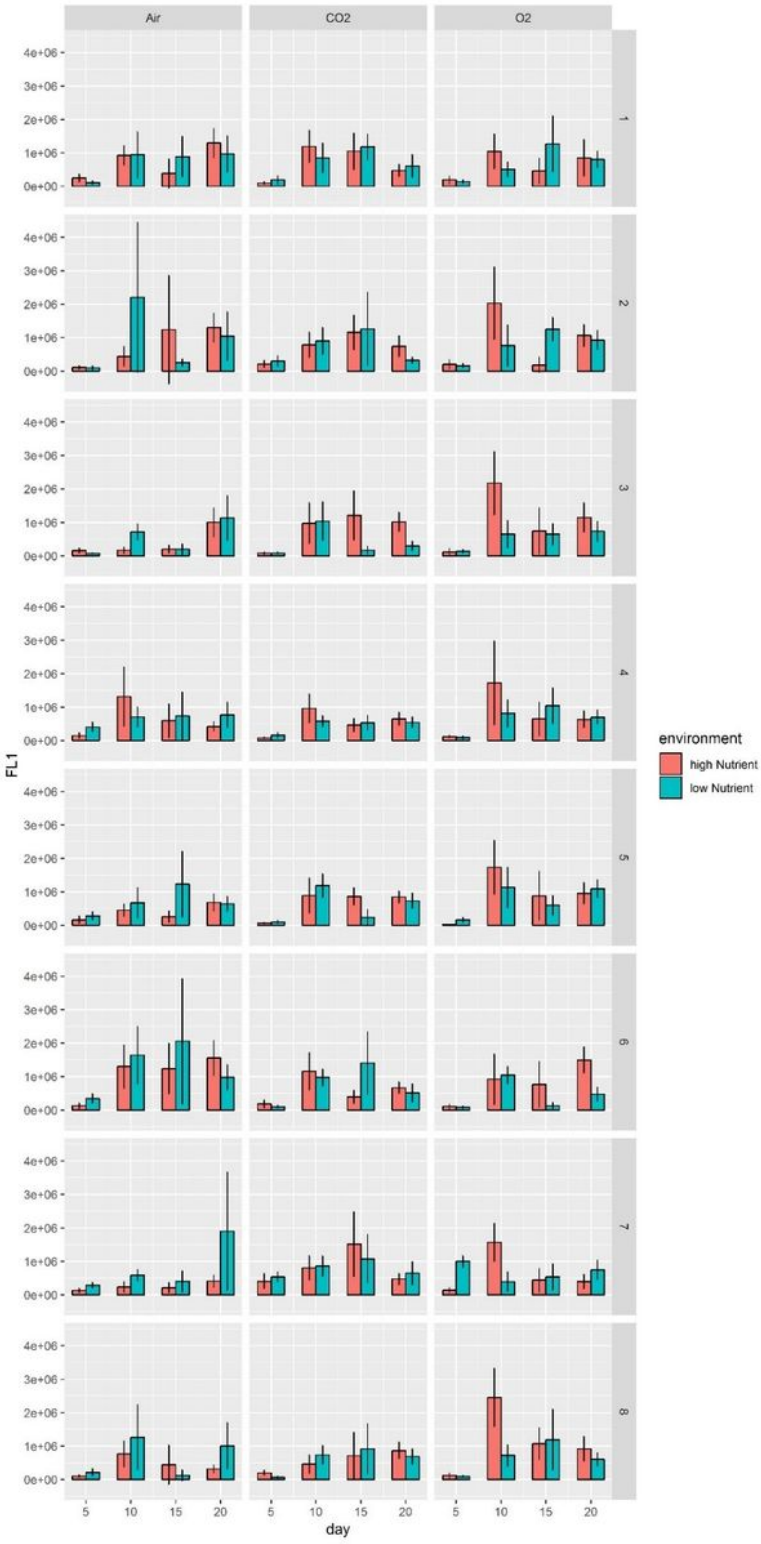

Figure 1

Comparisons of fluorescence intensities for eight probe hybridization activities of cells in the presence of oil under high- and low-nutrient conditions. The x-axis shows cultivation time, while the y-axis shows fluorescence intensity. The three treatments of air-ventilated, carbon dioxide-ventilated, and oxygen-ventilated conditions are shown as different vertical panels, while the eight horizontal sub-panels represent each of the eight gene probes. Red bars show values for high-nutrient conditions and blue bars

show those for low-nutrient conditions. Columns show average fluorescence intensities, and the error bars represent the 95% confidence interval. Gene 1: znuA, gene 2: phoB, gene 3: nqrF, gene 4: rubB, gene 5: znuB, gene 6: modA, gene 7: gltX, and gene 8: ectA.

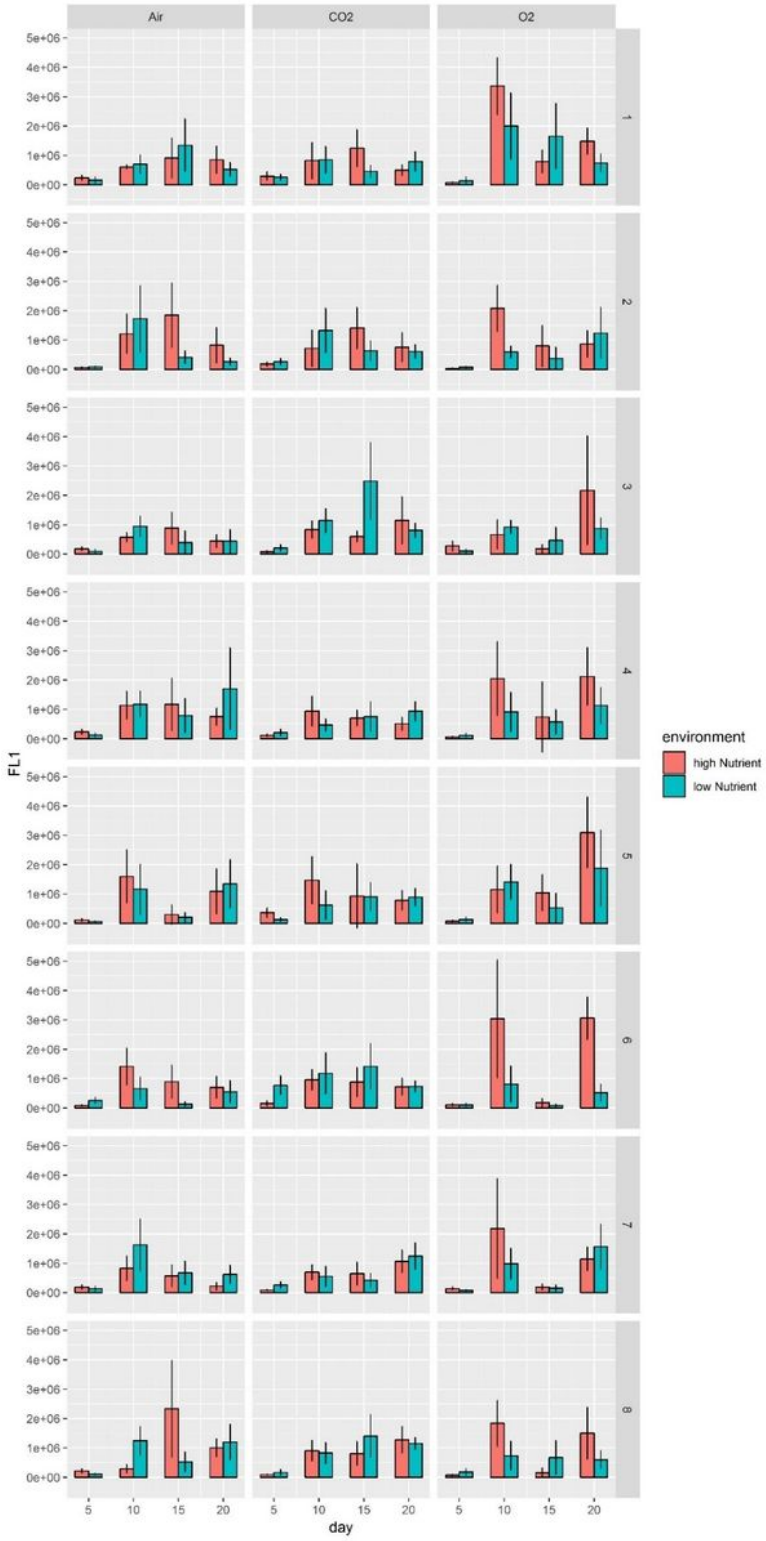

Figure 2

Comparisons of fluorescence intensities for eight probe hybridization activities of cells in the absence of oil under high- and low-nutrient conditions. The x-axis shows cultivation time, while the y-axis shows

fluorescence intensity. The three treatments of air-ventilated, carbon dioxide-ventilated, and oxygen-ventilated conditions are shown as different vertical panels, while the eight horizontal sub-panels represent each of the eight gene probes. Red bars show values for high-nutrient conditions and blue bars show those for low-nutrient conditions. Columns show average fluorescence intensities, and the error bars represent the 95% confidence interval. Gene 1: znuA, gene 2: phoB, gene 3: nqrF, gene 4: rubB, gene 5: znuB, gene 6: modA, gene 7: gltX, and gene 8: ectA.

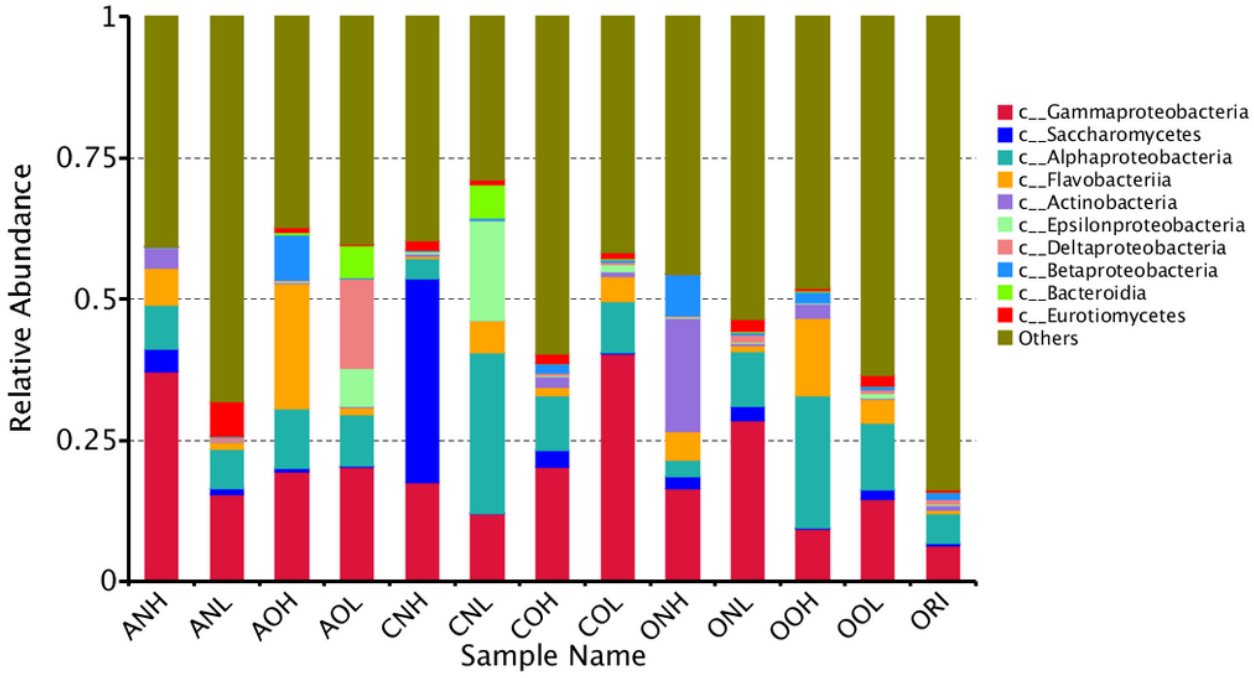

Figure 3

Taxonomic classifications of the culture communities based on the relative abundances of classes. Colors correspond to taxa indicated on the legend to the right and treatments are indicated at the bottom.

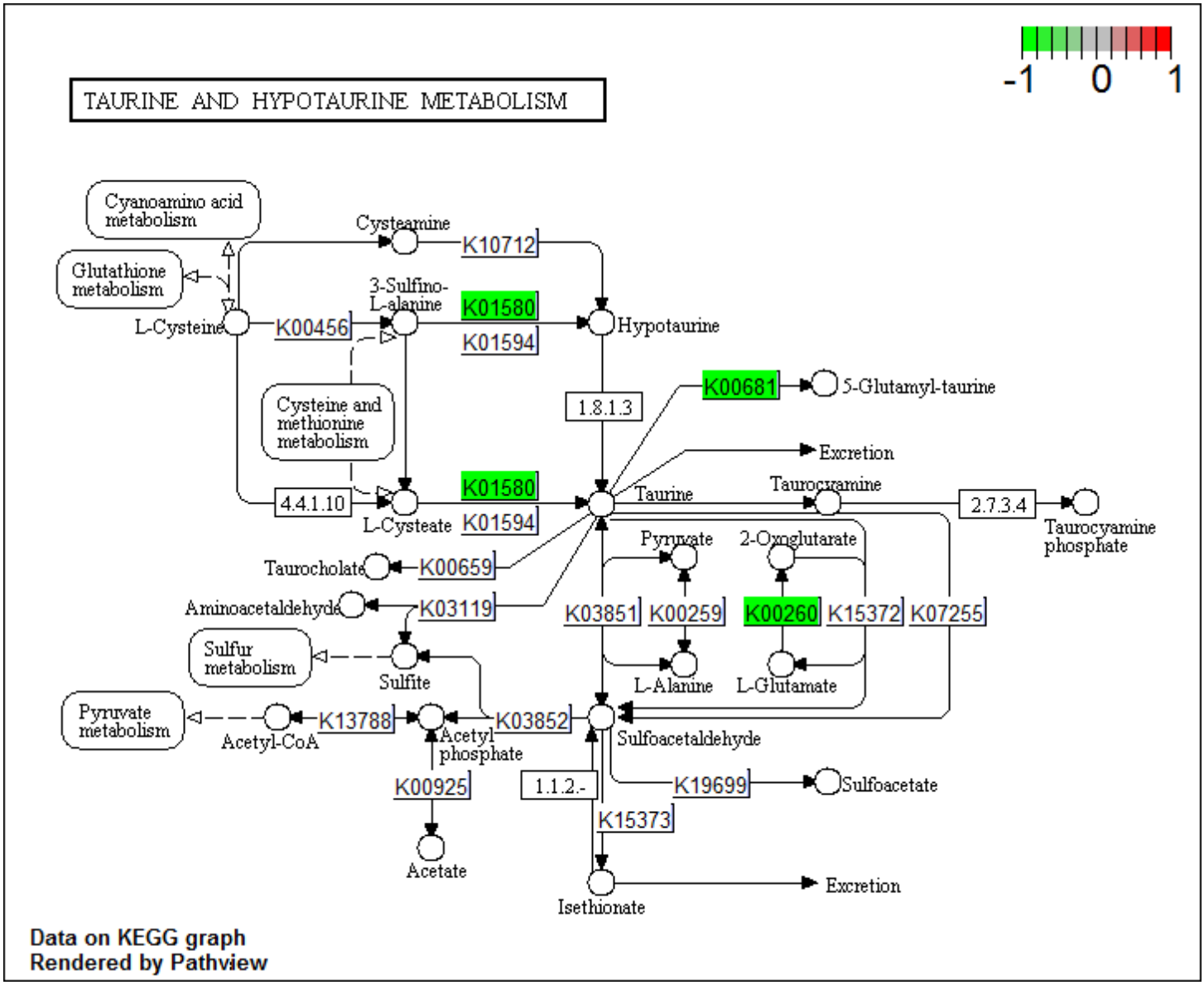

Figure 4

Taurine and hypotaurine metabolic pathways and differences in expression under the ANL vs ANH conditions. The color legend in the upper right corner indicates red values for level of gene upregulation and green for gene downregulation, as indicated for differentially expressed genes within the pathway map.

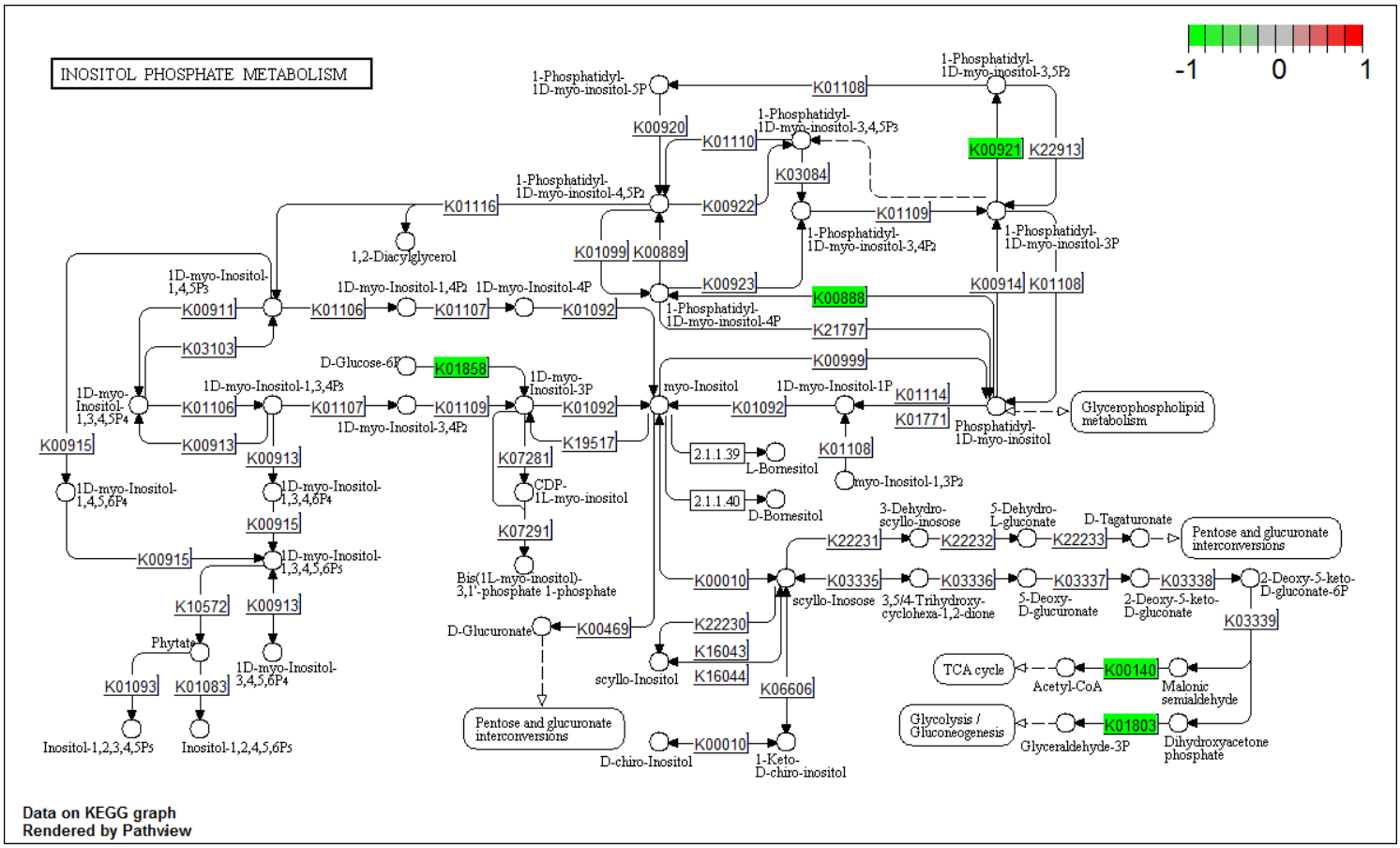

Figure 5

Inositol phosphate metabolic pathways and differences in expression under the ANL vs ANH conditions. The color legend in the upper right corner indicates red values for level of gene upregulation and green for gene downregulation, as indicated for differentially expressed genes within the pathway map.

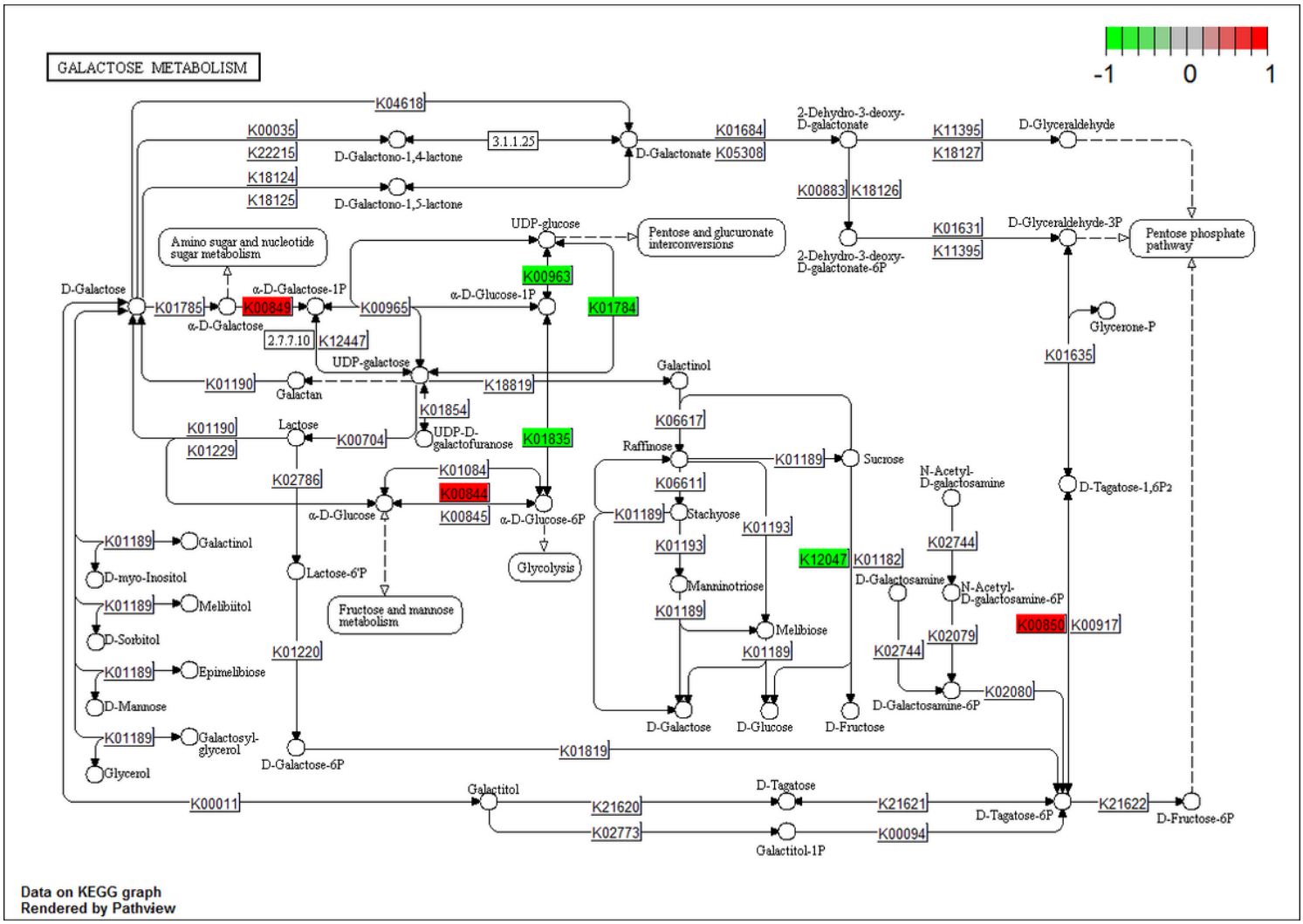

Figure 6

Galactose metabolic pathways and differences in expression under the CNH vs ANH conditions. The color legend in the upper right corner indicates red values for level of gene upregulation and green for gene downregulation, as indicated for differentially expressed genes within the pathway map.

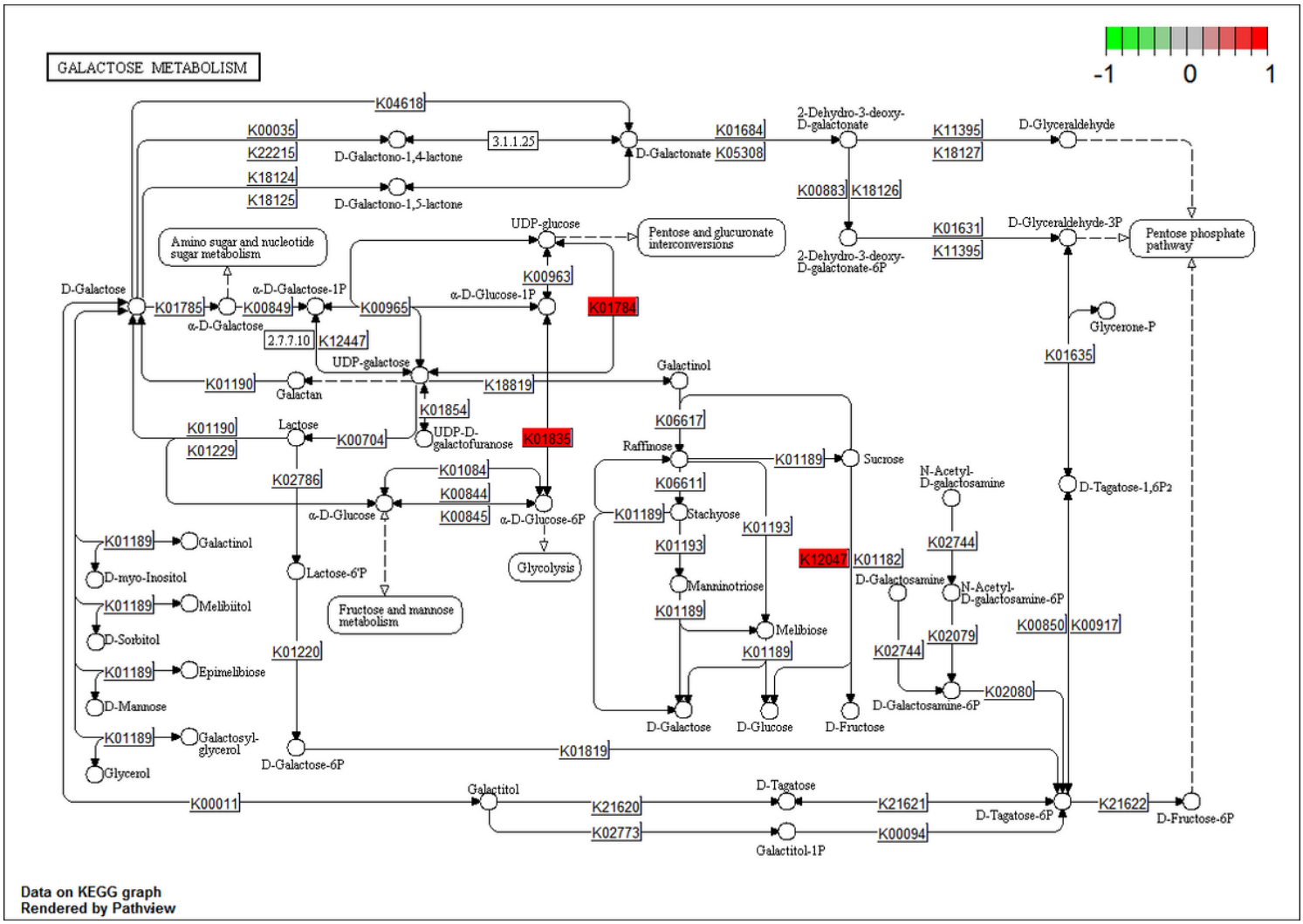

Figure 7

Galactose metabolic pathways and differences in expression under the ONH vs ANH conditions. The color legend in the upper right corner indicates red values for level of gene upregulation and green for gene downregulation, as indicated for differentially expressed genes within the pathway map.

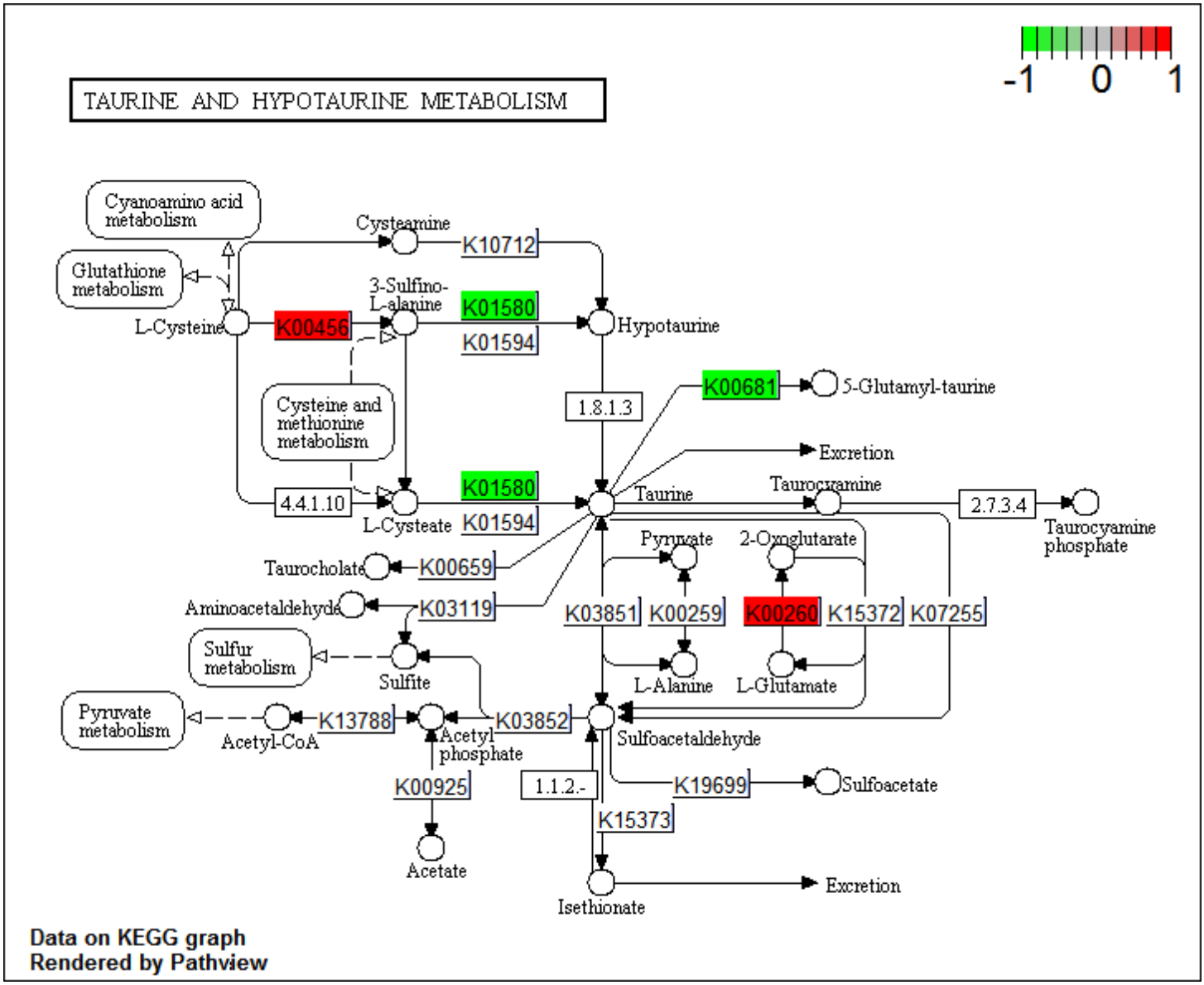

Figure 8

Taurine and hypotaurine metabolic pathways and differences in expression under the ONH vs ANH conditions. The color legend in the upper right corner indicates red values for level of gene upregulation and green for gene downregulation, as indicated for differentially expressed genes within the pathway map.

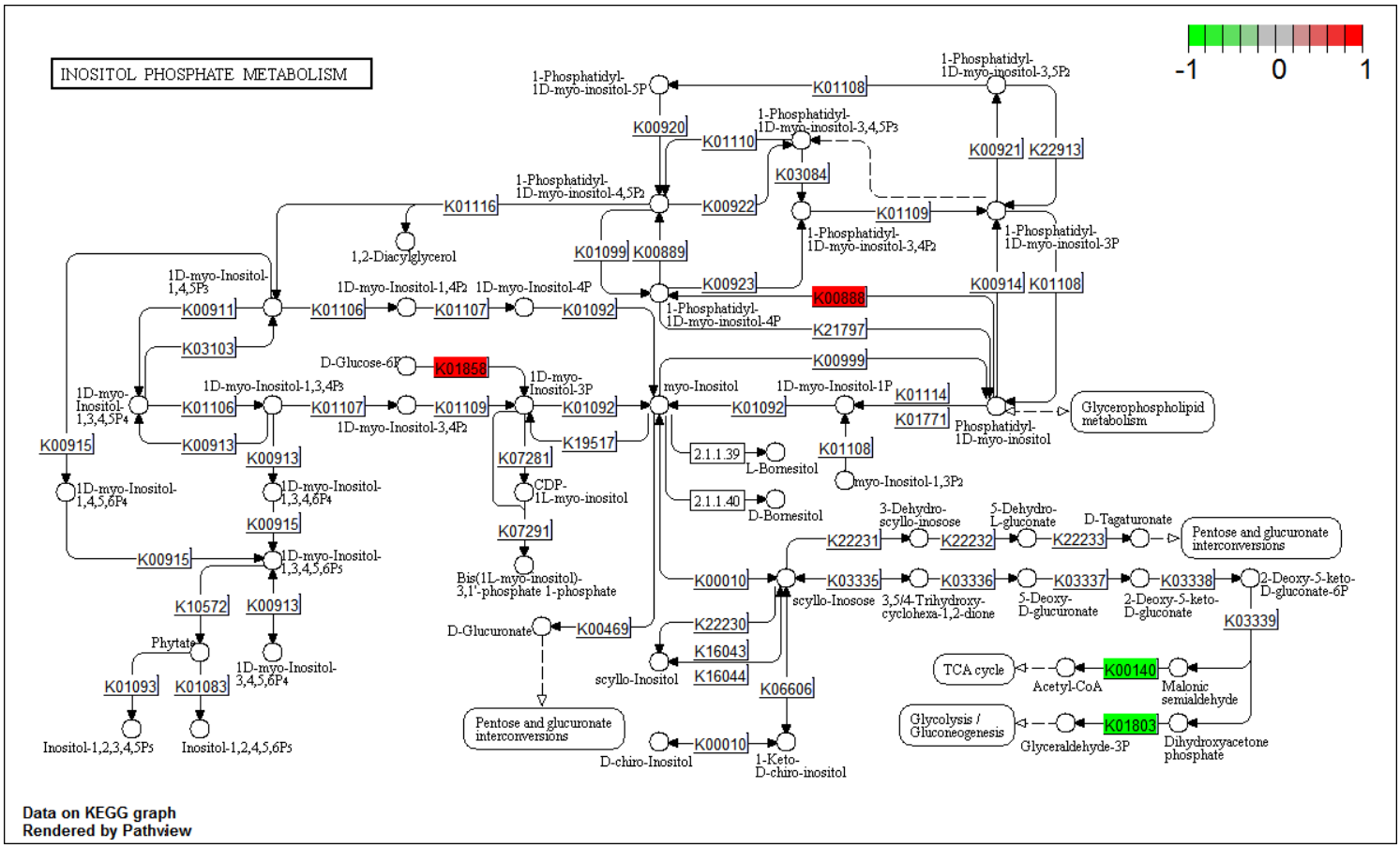

Figure 9

Inositol phosphate metabolic pathways and differences in expression under the COH vs OOH conditions. The color legend in the upper right corner indicates red values for level of gene upregulation and green for gene downregulation, as indicated for differentially expressed genes within the pathway map.

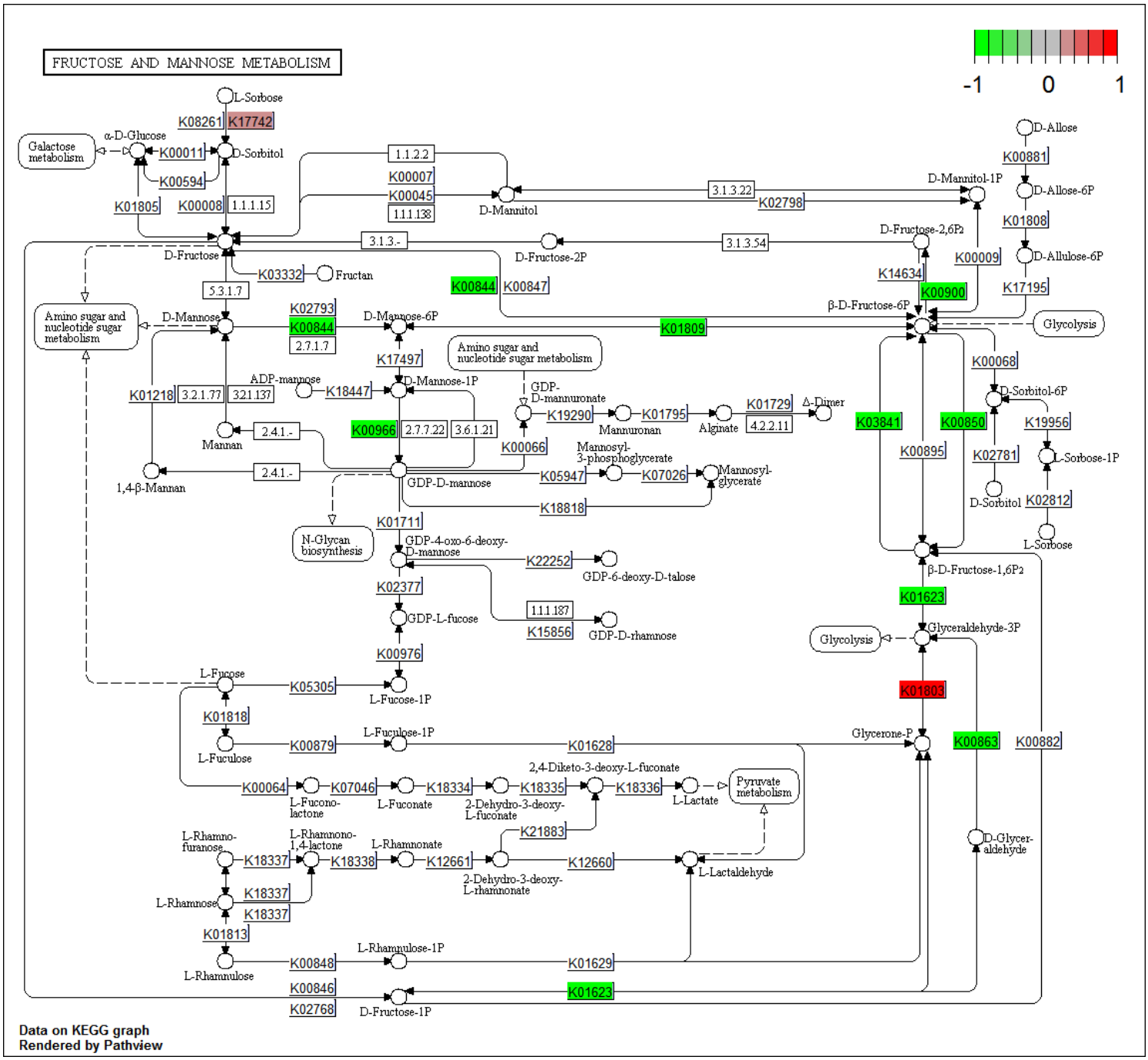

Figure 10

Fructose and mannose metabolic pathways and differences in expression under the COH vs CNH Conditions. The color legend in the upper right corner indicates red values for level of gene upregulation and green for gene downregulation, as indicated for differentially expressed genes within the pathway map.

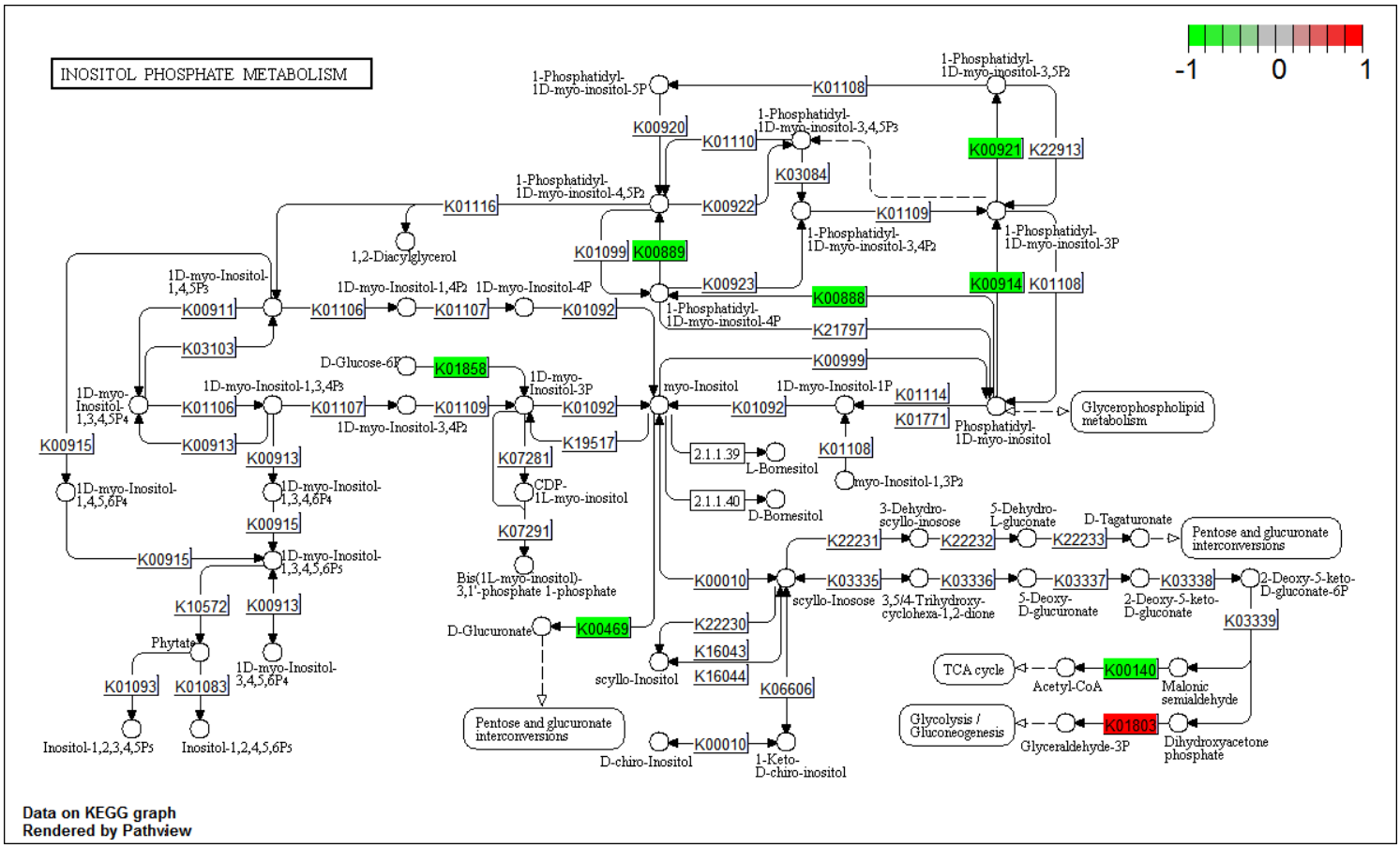

Figure 11

Inositol phosphate metabolic pathways and differences in expression under the COH vs CNH Conditions. The color legend in the upper right corner indicates red values for level of gene upregulation and green for gene downregulation, as indicated for differentially expressed genes within the pathway map.